J. exp. Biol. ***193****, 139–156 (1994)*
Printed in Great Britain © The Company of Biologists Limited 1994

POWER OUTPUT OF SCALLOP ADDUCTOR MUSCLE DURING CONTRACTIONS REPLICATING THE *IN VIVO* MECHANICAL CYCLE

RICHARD L. MARSH AND JOHN M. OLSON*

Department of Biology, Northeastern University, 360 Huntington Avenue, Boston, MA 02115, USA

Accepted 7 April 1994

Summary

Because measurements on isolated skeletal muscles are often made with limited knowledge of *in vivo* kinematics, predictions of mechanical performance during natural movements are subject to considerable uncertainties. We used information on the *in vivo* length cycle and phase of activation of the scallop adductor during swimming at 10 °C to design an *in vitro* contractile regime that replicated the natural cycle. Replicating the *in vivo* length cycle and stimulation regime resulted in power output during cyclic contractions that matched *in vivo* performance both qualitatively and quantitatively. When sinusoidal length changes were used instead of the natural length trajectory, the adductor muscle produced a similar average power output (approximately 30 W kg^{-1} at 1.9 Hz), but the distribution of power throughout the cycles was quite different. We examined the instantaneous force–velocity properties during cyclic contractions and found that the muscle operated on or near its isotonic force–velocity curve for only 30–40 % of the time required for shortening. During sinusoidal length cycles, the force–velocity trajectory was quite different. We conclude that during cyclic contractions the isotonic force–velocity curve of skeletal muscle sets an approximate boundary to the force–velocity trajectory, but the shape of this trajectory, and thus the distribution of power output, depends on the pattern of length change.

Introduction

The ability to produce mechanical power sets limits on the locomotor performance of animals, and thus has been used as a major measure of muscle performance (Hill, 1950; Wilkie, 1959; Weis-Fogh and Alexander, 1977; McMahon, 1984; Josephson, 1985; Jones *et al.* 1986; Josephson and Stokes, 1988; Rome, 1990). However, the underlying assumptions of many of these discussions are based on measurements made on muscles under simplified *in vitro* loading conditions, and their usefulness in predicting power output during complex movements *in vivo* remains largely untested. For example, the

*Present address: Biology Department, Villanova University, Villanova, PA 19085, USA.

Key words: cyclic contraction, power output, muscle contraction, force–velocity curve, scallop, *Argopecten irradians.*

isotonic force–velocity curve certainly reflects an important intrinsic property of the contractile elements, but the measurement of a particular shortening velocity *in vivo* should not be used to predict that the muscle is operating at a specified point on the isotonic force–velocity curve. The transient nature of activation *in vivo* coupled with the effects of the length history make this prediction open to question. A. V. Hill's question, 'Is the [isotonic] force–velocity relation an instantaneous property of muscle?' (Hill, 1970) has still not been thoroughly addressed with regard to the conditions under which natural movements occur. Models of contraction incorporating multiple parameters have been developed (e.g. van Leeuwen, 1992), and such models will benefit from more extensive knowledge of how muscles move *in vivo* and the power output under these conditions.

To bring *in vitro* measurements closer to the reality of *in vivo* function, a series of recent investigations has used a technique pioneered by Machin and Pringle (1960) for fibrillar flight muscle in insects. In this technique, muscles are subjected to sinusoidal length changes and power output is optimized by varying several experimental parameters (e.g. Josephson, 1985; Josephson and Stokes, 1988; Altringham and Johnston, 1990; Stevenson and Josephson, 1990). This method provides a standard way of comparing muscles in repetitive shortening contractions and includes the influences of shortening and deactivation/activation cycles on average mechanical power. However, this technique incompletely bridges the gap between *in vitro* and *in vivo* studies. First, the sinusoidal length cycle is arbitrary and probably accurately reflects the *in vivo* cycle for only a limited set of locomotor muscles. Second, the attempt to optimize power output, although useful as a standard for comparing muscles, begs the question of whether or not power is actually optimized *in vivo*.

We used our recent measurements of the precise pattern of movement of the adductor muscle of scallops during jet-propulsion swimming (Marsh *et al.* 1992) to design a series of measurements that replicates *in vitro* the mechanical cycle found during swimming. Reproducing the *in vivo* length cycle incorporates the strengths of the cyclic contraction technique in measuring power output in repetitive contractions and overcomes the problems mentioned above. The scallop adductor provides an ideal first test of this technique as the following can be measured with precision during natural locomotion: (1) the cycle of length change, (2) the pattern of stimulation, and (3) the power output. The first and second of these *in vivo* measurements are necessary to design the *in vitro* measurements. The third allows a test of the adequacy of the *in vitro* measurements for estimating *in vivo* performance.

During jet-propulsion swimming, scallops propel themselves using the striated portion of their single adductor muscle (Dakin, 1909; Yonge, 1936; Lowy, 1954; Mellon, 1969; Wilkens, 1981; Marsh *et al.* 1992). The bulk of the large adductor in these animals is striated. The smooth portion is anatomically discrete and is used for slow movements or to maintain the valves in a fixed position (Wilkens, 1981). The simple morphology of these animals allowed Marsh *et al.* (1992) to measure the muscle length change and pressure in the mantle cavity simultaneously and to calculate the mass-specific power output of the adductor muscle with a time resolution of a few milliseconds. In the present study, we have also recorded electromyograms (EMGs) to determine the phase of stimulation relative to the length change.

Materials and methods

Statistics

Average values are given in the text as the mean ± S.E.M. The non-parametric Mann–Whitney *U*-test was used to compare the *in vivo* and the *in vitro* values, because of significant differences in the variance between the two groups.

Animals

Argopecten irradians (Lamarck) were supplied by the Department of Marine Resources, Marine Biological Laboratories, Woods Hole, MA, and maintained in artificial sea water at 10 °C for a maximum of 14 days before use. The nine animals used were restricted in size to within the range of sizes on which performance had been measured previously (Marsh *et al.* 1992). The mean body mass was 27±1.7 g including the valves, but with the mantle emptied of sea water. The mean shell dimensions, measured as the maximum value in each direction, were: dorsal–ventral, 52.7±0.9 mm; anterior–posterior, 55.8±1.5 mm; left–right, 22.4±0.5 mm.

In a series of experiments, we noted an apparent seasonal change in force production by our preparations of adductor muscle. Forces were about 25 % lower in animals received between January and April compared with those received from 15 May to 15 September. Force was stable during this latter period. As these animals were received in separate shipments from variable collecting localities, we cannot rule out effects other than seasonal ones. Our previous work on *in vivo* performance of the adductor muscle took place between 29 August and 7 September. The *in vitro* experiments reported here took place between 20 May and 26 July.

Electromyograms

Electromyograms were recorded from the striated portion of the adductor muscle by inserting bipolar electrodes fashioned from 0.076 mm stainless-steel wire into the muscle through a fine hole drilled in the left (top) valve. Signals were amplified by WPI model DAM-50 preamplifiers with high- and low-pass filters set at 10 and 3000 Hz, respectively. Muscle length was recorded simultaneously with a Triton Technology model 120 Sonomicrometer (Marsh *et al.* 1992). Data were acquired digitally with a sampling frequency of 1200 Hz using MacAdios II 12-bit A/D converters operating in a Macintosh II microcomputer.

Muscle preparations

The muscle preparation consisted of a small bundle of fibers from the anterior edge of the adductor muscle. The muscle bundle was dissected at 0 °C and left attached to pieces of the valves at each end (Olson and Marsh, 1993). Following dissection, the preparation was firmly secured at one end to the bottom of a Lucite chamber. The other end was attached to the lever of a Cambridge Technology model 305 ergometer *via* a harness fashioned from light-weight silver chain. The preparation was suspended in a bath of temperature-controlled Ringer (Olson and Marsh, 1993) saturated with 100 % oxygen. Supramaximal stimuli of 0.5 ms duration were generated by a Grass model S48

stimulator, amplified by a d.c. power amplifier, and delivered to the fiber bundle *via* platinum plate electrodes running the full length of the muscle on either side.

These preparations were a subset of those on which we previously reported isometric and isotonic contractile properties (Olson and Marsh, 1993). The nine preparations used in the present study had a mean mass of 0.24±0.1 g and an optimal length for twitch force production (L_0) of 27.35±0.78 mm. They produced a mean twitch force of 22.6±0.6 N cm^{-2} with a twitch to tetanus ratio of 0.880±0.014.

Contractile measurements

Cyclic contraction experiments were controlled by outputs from a MacAdios II data acquisition system (GW Instruments) controlled by Superscope software operating in a Macintosh II computer. Data outputs on two channels and inputs on two channels to the MacAdios board were simultaneous (not multiplexed). The stimulator was controlled by a digital control signal and the muscle length was controlled by an analog signal generated by a 16-bit D/A converter. The length-control signal produced four cycles in each series. We used two types of cycles of muscle length; sinusoidal and natural, replications of the *in vivo* cycle. Sine waves were generated by Superscope software and scaled to the appropriate frequency and muscle strain. The complex nature of the *in vivo* length changes during swimming made construction of a *de novo* length-control signal that matched the *in vivo* pattern impractical. Therefore, we used an actual length trace recorded from one of our experimental animals. The trace used was chosen because it had close to the mean value for cycle time, excursion, and maximum and average velocities during adduction and abduction. The sonomicrometer data had a very high signal to noise ratio (e.g. Fig. 1). Nevertheless, we eliminated the low-level noise from the control signal by fitting overlapping polynomial regressions to segments of the trace using the program Igor (WaveMetrics). The differential of the fitted curve was examined to ensure that the overlapping segments did not produce any discontinuities and that the velocity matched the *in vivo* data.

Force and position were simultaneously recorded by 12-bit A/D converters with a sampling frequency of 1200 Hz. Calculations on the acquired data were carried out with Superscope from GW Instruments and Igor from WaveMetrics. Owing to a slight under-regulation of the lever with a rapidly changing force, a small artifact appeared on the length and velocity traces at the beginning of the shortening cycle (see Figs 2 and 5). This artifact was largest on the first cycle when the lever had been held statically, but even in this cycle it occurred while the force was quite small and it had no significant influence on the calculated power output.

The striated adductor muscle of scallops is quite fatigable (Marsh *et al.* 1992; Olson and Marsh, 1993). Obtaining high initial forces required dissection at a low temperature. Following dissection, the fiber bundles were allowed to rest for approximately 1 h after suspension in Ringer at approximately L_0. The first contractions after the rest were performed isometrically. The force in the subsequent cyclic contractions was corrected for fatigue by measuring isometric force at intervals throughout the experimental series. After applying this correction, the same mechanical conditions resulted in similar calculated power output at the beginning and end of the series of contractions. A similar

correction has been applied in other experiments with cyclic contractions (Stevenson and Josephson, 1990).

Results

Electromyograms

The EMG in scallop adductor results from a extracellularly recorded end-plate potential (Mellon, 1968) with prominent low-frequency components (Fig. 1). The EMGs were interpreted as consisting of a single stimulus in most cycles. However, the shape varies from cycle to cycle and as many as three stimuli may be given in a few cycles. The electromechanical delay, measured as the time from the start of the EMG to the beginning of adduction, was 28±1.3 ms at 10 °C. On the basis of these data, we used a single stimulus in each cycle of our *in vitro* experiments. In experiments with isolated fiber bundles, power output varied only slightly and not in a consistent manner among different preparations when the number of stimuli was increased from 1 to 4 (R. L. Marsh and J. M. Olson, unpublished observations).

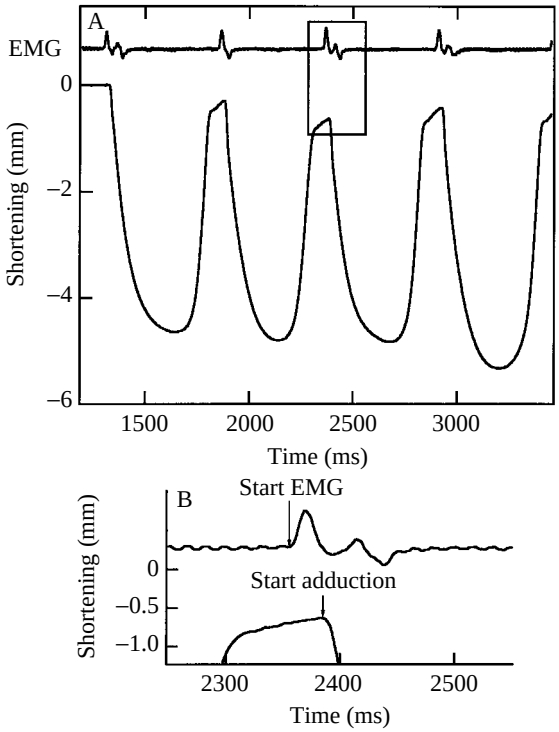

Fig. 1. Representative record of muscle shortening (from the sonomicrometer) with a simultaneously recorded electromyogram (EMG) in the adductor muscle of *Argopecten irradians*. (A) Four sequential valve claps at the beginning of a swim. The box at the beginning of the third adduction indicates the area expanded in B. (B) Amplified view of the EMG and length trace at the beginning of the third adduction. The electromechanical delay was measured as the time from the start of the EMG to the beginning of adduction.

Replication of the in vivo *shortening cycle*

The information gathered on the function of the muscle *in vivo*, together with the simple mechanics of the scallop locomotor system, accurately defines the parameters necessary for replicating the *in vivo* mechanical cycle (Fig. 2). The initial length was set

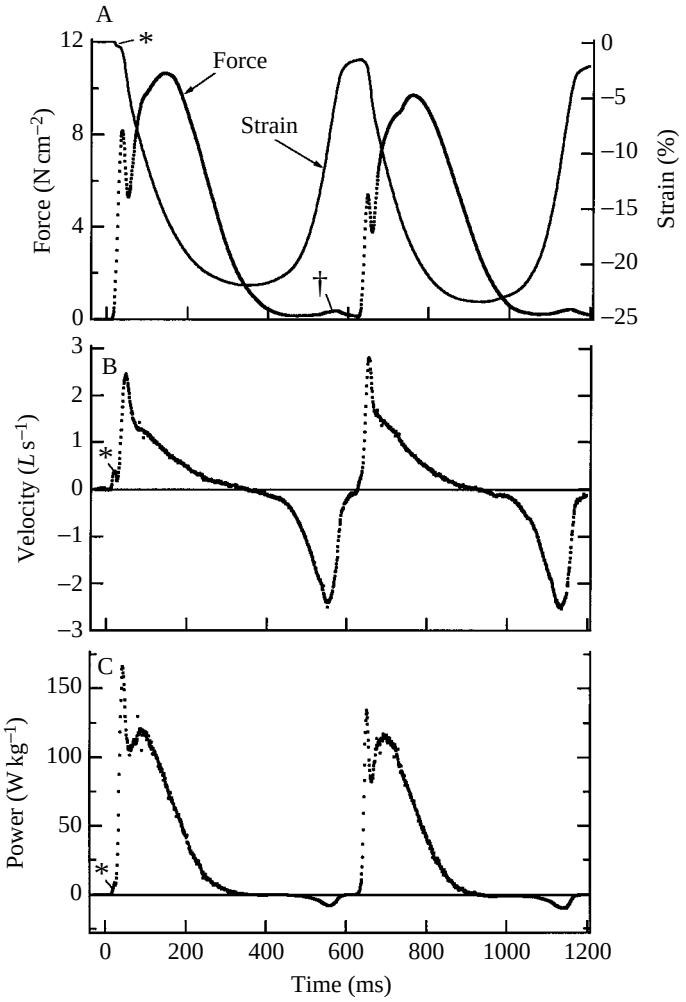

Fig. 2. Contractions of a bundle of muscle fibers from the adductor muscle of *Argopecten irradians*. The length of the muscle and timing of stimulation were controlled by computer and reflect *in vivo* conditions during swimming (Marsh *et al.* 1992). The single stimulus in each cycle was given 28 ms before the beginning of shortening. A small artifact (*) due to underregulation of the lever occurs when force rises rapidly at the beginning of the first cycle. This artifact has almost no effect on power output. (A) Simultaneous records of muscle length change, plotted as strain (percentage change in length from the starting length), and force output per cross-sectional area. The force during rapid lengthening remained quite low (†), indicating a low inherent viscosity of the relaxed muscle. (B) Shortening velocity calculated by numerically differentiating the length record. (C) Power calculated as the product of force and velocity.

at $1.4L_{cl}$, where L_{cl} is the length of the muscle at its anterior edge with the valves completely closed. The value of $1.4L_{cl}$ corresponds to the mean maximum length of the anterior portion of the striated adductor muscle found during swimming at 10 °C (Marsh *et al.* 1992). This length is also very close to the length for optimal force production in isometric twitches (L_0). Olson and Marsh (1993) found the mean L_0 to be $1.38\pm0.01L_{cl}$ (N=19). The mean percentage strain *in vivo* at 10 °C during the first four shortening cycles was 22.5 % of the initial length. The timing of the single stimulus was kept constant at a value equal to the mean electromechanical delay measured *in vivo* (Fig. 1). We varied the cycle time to allow for differences in the twitch time among muscle preparations. The appropriate cycle time was chosen on the basis of the residual force present at the end of shortening, because muscle lengthening during natural swimming cannot begin until the torque produced by the adductor muscle drops to a value equal to that in the opposing elastic hinge. [We estimated the static torque of the hinge as well as the possible error due to rapid compression (R. L. Marsh and J. M. Olson, unpublished observations).] The contractile frequencies used *in vitro* (1.57–1.89 Hz; mean 1.71 Hz) were similar to those found during the first four cycles of natural swimming (1.62–1.97 Hz; mean 1.76 Hz) (Marsh *et al.* 1992).

Fig. 2 shows representative data collected at 10 °C. Because muscle length was controlled by input to the ergometer, the change in shortening velocity throughout each cycle (Fig. 2B) mirrored events occurring *in vivo* (Marsh *et al.* 1992). Force (Fig. 2A) initially rose sharply and then fell in response to the rapidly increasing shortening velocity. The first peak in force corresponded approximately to the maximum acceleration of the lever. During lengthening, very little force was required to re-extend the muscle. The very small transient increase in force during rapid lengthening indicates that the inherent viscosity of the relaxed adductor muscle was quite low. Forces due to passive elasticity were minimal over the range of lengths used. Power output (Fig. 2C), calculated as the product of velocity and force, had an initial peak during the period of rapidly increasing velocity and a second more sustained peak that corresponded to the time when the propulsive jet is active *in vivo*.

The kinetics of force during these shortening contractions was quite different from that measured during isometric twitches (Olson and Marsh, 1993) (Fig. 3). The shorter twitch during shortening is not accounted for solely by length–tension effects (Olson and Marsh, 1993) and presumably reflects the importance of shortening-dependent deactivation (Edman, 1980; Housmans *et al.* 1983; Josephson and Stokes, 1988). The presence of shortening-dependent deactivation in a muscle regulated by Ca^{2+} binding to myosin (Lehman and Szent-Györgyi, 1975) is intriguing as length-dependent changes in Ca^{2+} binding to the thin filament have been suggested as a possible mechanism for this deactivation in vertebrate striated muscle (Edman, 1980; Housmans *et al.* 1983). Functionally, the shortened twitch would allow re-extension to occur earlier during swimming than would be predicted on the basis of the isometric kinetics (Olson and Marsh, 1993).

To compare quantitatively the average performance *in vivo* and *in vitro*, we calculated the average work, total power and peak power produced during the first and second cycles for all preparations (Fig. 4). (Cycles 3 and 4 were similar to cycle 2.) The mean values

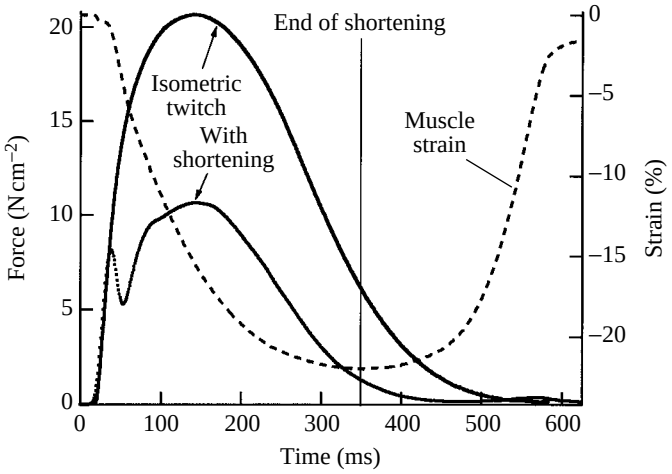

Fig. 3. Comparison of force produced by the adductor muscle of *Argopecten irradians* in an isometric twitch with that recorded during the first cycle of a simulated swim (see Fig. 2). The stimulus in each case occurred at time zero. The dashed line shows muscle strain during the simulation.

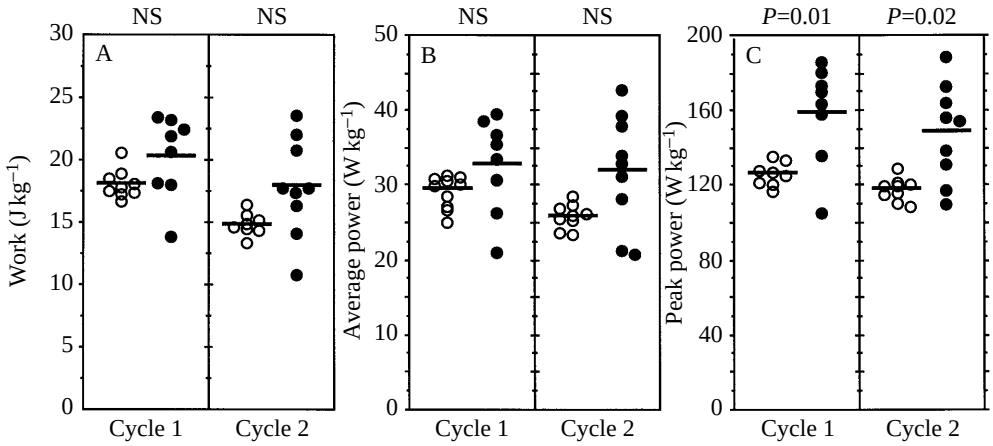

Fig. 4. Comparison of (A) total work, (B) average power and (C) peak power output of the adductor muscle of *Argopecten irradians* during the first two cycles of jet-propulsion swimming (●) (Marsh *et al.* 1992) with that recorded in the same cycles *in vitro* (○) under conditions that replicate those found *in vivo*. The peak power given is that during the jet-propulsion phase *in vivo* or the equivalent phase *in vitro*. The symbols are individual values. The horizontal lines indicate the mean values for each group. The *P*-values given are the two-tailed probabilities based on the Mann–Whitney *U*-test. NS, not significant, $P>0.05$.

found *in vitro* for these variables were lower than the corresponding *in vivo* values (mean difference approximately 16 %). However, given the variability in the *in vivo* values, the differences for average power and work were not statistically significant (Mann–Whitney *U*-test, $P>0.05$).

Sinusoidal shortening cycles

The present report concentrates on contractions that replicate the *in vivo* shortening cycle; however, for comparison with previous studies of other skeletal muscles, we explored performance during sinusoidal shortening cycles (Fig. 5). We recorded performance during sinusoidal length changes in four preparations, for which we had already recorded performance during contractions replicating the *in vivo* shortening

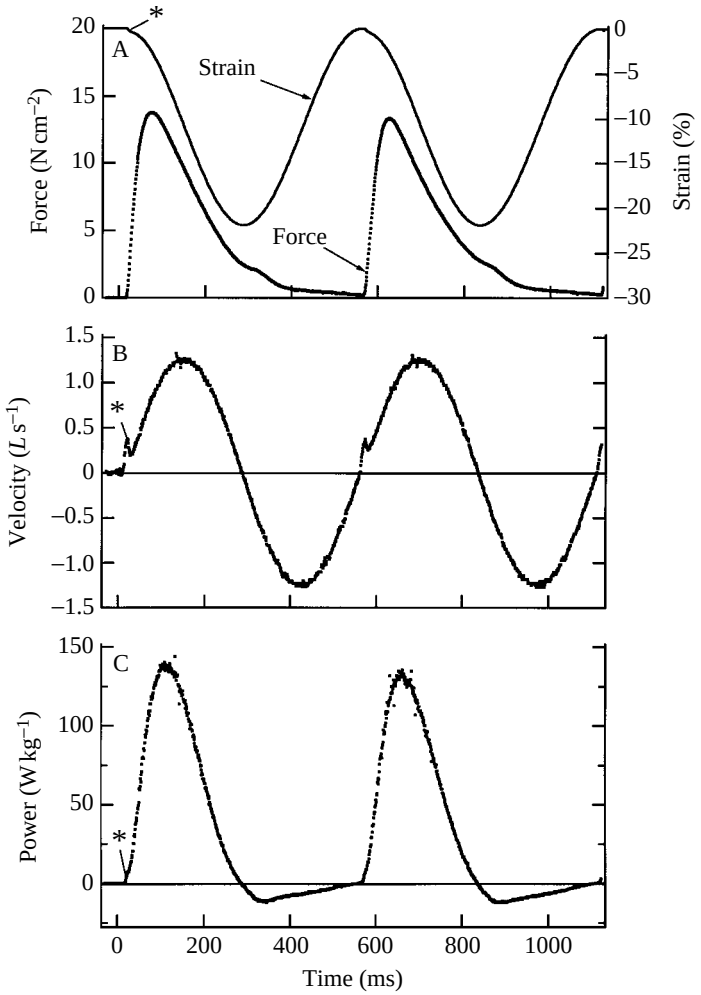

Fig. 5. Contractions of a bundle of muscle fibers from the adductor muscle of *Argopecten irradians* during sinusoidal changes in length. The length of the muscle and timing of stimulation were controlled by computer. A small artifact (*) due to underregulation of the lever occurs when force rises rapidly at the beginning of each cycle. This artifact has almost no effect on power output. (A) Simultaneous records of muscle length change, plotted as strain (percentage change in length from the starting length), and force output per cross-sectional area. (B) Shortening velocity calculated by numerically differentiating the length record. (C) Power calculated as the product of force and velocity.

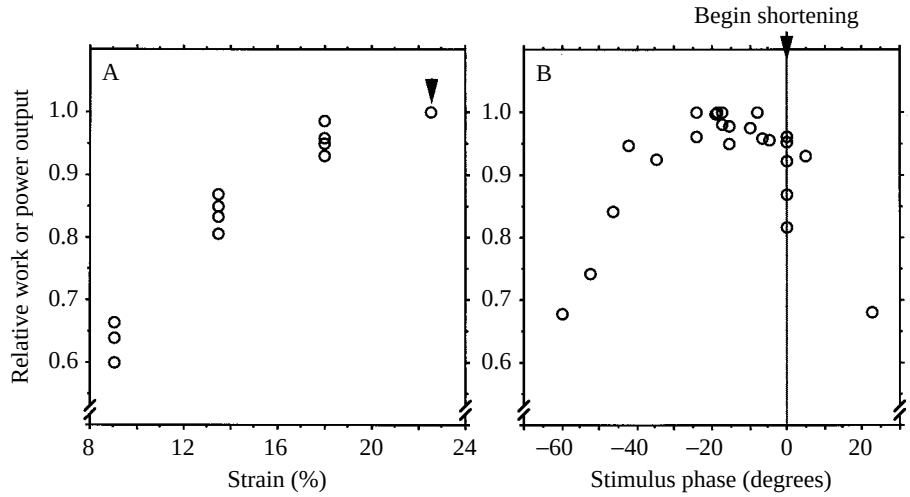

Fig. 6. Effects of (A) strain and (B) stimulus phase on power or work output of the adductor muscle of *Argopecten irradians* averaged over the first complete cycle of sinusoidal shortening. Power is expressed as a fraction of the maximum power recorded in each series. Stimulus phase was defined as the difference in degrees (complete cycle=360 ˚) between the stimulus and the beginning of shortening. Strain is defined as the maximum (peak-to-peak) percentage length change during a complete cycle. Starting length was $1.4L_{cl}$, which is approximately equal to L_0 (see text). For each preparation, the frequency was constant and varied from 1.7 to 2.2 Hz among preparations (mean 1.9 Hz). The arrowhead in A marks a point where four values are superimposed.

cycle. Using sine-waves, we explored the effects of stimulus phase, strain and frequency. (Strain here refers to the maximum length change during the cycle.) The highest average power for a complete cycle was always obtained at a strain matching the average *in vivo* strain, 22.5 % (Fig. 6A). We kept the starting length constant at $1.4L_{cl}$ because initial work with this muscle indicated that it was easily damaged when stretched to long lengths. Optimal power output occurred when the single stimulus was given at a mean of 24.5±4.8 ms before the start of shortening. Stimulus phase can be defined in degrees relative to one complete cycle, which is set as equal to 360 ˚ with the beginning of shortening designated as 0 ˚. The optimal phase was −17 ˚ (Fig. 6B). Given the twitch properties of the scallop adductor (Olson and Marsh 1993), this phase corresponds to a value of about 23 ˚ as defined by Josephson (1985). The optimal frequency, given the above values of strain and phase, was 1.9±0.1 Hz.

The work output in natural and sinusoidal cycles was similar (Table 1). Power output was slightly higher in the sinusoidal cycles, in part because the optimal frequency was higher than the frequency that best mimicked the *in vivo* conditions. In the four muscle preparations for which we have data on both types of cycles, average power outputs at 10 ˚C were 34.1±1.0 and 29.1±1.0 $W\,kg^{-1}$ during sinusoidal and natural cycles, respectively. However, this power was distributed differently during the cycle (Fig. 7), resulting in a distinctly different work loop (Fig. 8). The force peak during shortening is narrower during sinusoidal cycles than during natural cycles (Figs 2 and 5).

Table 1. *Comparison of performance in natural and sinusoidal cycles in four preparations*

Cycle type	Frequency (Hz)	Average power ($W\,kg^{-1}$)	Peak power ($W\,kg^{-1}$)	Work ($J\,kg^{-1}$)	Maximum stress ($N\,cm^{-2}$)
Sinusoidal	1.92±0.11	34.1±1.0	150.7±4.0	17.8±0.66	14.4±0.5
Natural	1.82±0.11	29.1±1.0	135.8±7.2	16.5±0.88	10.9±0.5
*P**	0.0001	0.02	0.03	0.2 (NS)	0.0001

*Paired *t*-test; NS, not significant.

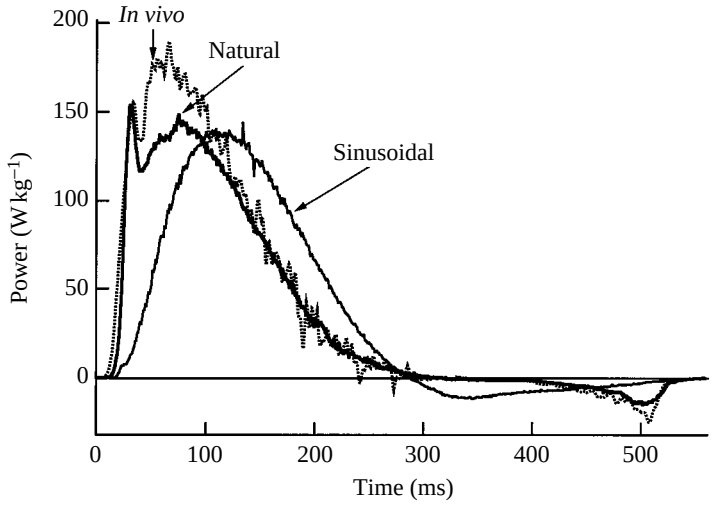

Fig. 7. Comparison of power output of the adductor muscle of *Argopecten irradians* during the first cycle of jet-propulsion swimming (Marsh *et al.* 1992) (labelled *In vivo*) with that recorded in the same cycle *in vitro* during contractions that replicate those found *in vivo* (labelled Natural) and during sinusoidal changes in length (labelled Sinusoidal).

Discussion

Comparison of performance in vitro *and* in vivo

Did the *in vitro* contractions accurately model the *in vivo* power output of the adductor muscle during swimming? This comparison can be evaluated in terms of both the temporal correspondence and the quantitative agreement between the *in vivo* and *in vitro* data. First, the time course and distribution of power output throughout the cycle were remarkably similar under the two conditions (Fig. 7). The only difference in the relative distribution of power calculated from the *in vivo* and *in vitro* data was the size of the initial brief peak. This initial peak of *in vitro* power output is related to the high force produced during the initial phase of acceleration. The force and power then quickly decline because of the increasing contractile speed (see also Fig. 9). Force and power output increase again as the lever decelerates, corresponding to the time *in vivo* when the mantle edges seal and the propulsive jet is formed (Marsh *et al.* 1992). In contrast to the

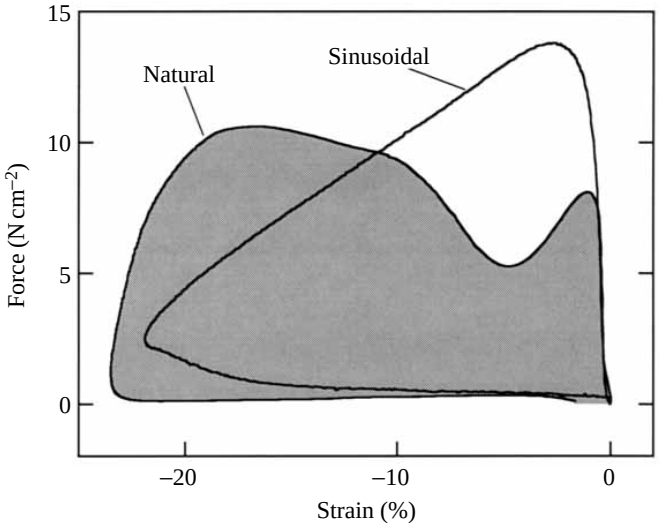

Fig. 8. Work loops (muscle force *versus* strain) for the adductor muscle of *Argopecten irradians* during cycle 1 of representative natural and sinusoidal cycles. Net work during the complete cycle is proportional to the enclosed area (Josephson, 1985).

in vivo estimates, the magnitude of the first peak during *in vitro* contractions often exceeded the maximum value found during the more sustained second peak (Figs 2 and 4). The work done during this first peak represented a very small portion of the total work output of the adductor muscle. Nevertheless, the adduction simulated *in vitro* possibly uncovered components of the force input required *in vivo* that were not measured directly by Marsh *et al.* (1992); for example, the force required to accelerate the added mass and/or nonlinear viscoelastic forces during rapid compression of the hinge.

The performance of our *in vitro* preparations resembled that predicted from *in vivo* data during lengthening as well as during shortening. Force at the end of shortening behaves as might be expected *in vivo* given the mechanics of swimming. Re-extension of the muscle during swimming would be expected to begin as the force in the muscle drops below that produced by the elastic hinge. The velocity of lengthening would then increase as the force declined further, with the maximum velocity being determined by the hydrodynamics of valve movement. The *in vitro* data match these expectations. These data show that controlling length and stimulation pattern is sufficient to replicate most features of *in vivo* performance.

How well do the data obtained *in vivo* and *in vitro* agree quantitatively? Because of individual variation among preparations, this question is best answered by comparing data from several preparations (Fig. 4). The work and power produced *in vitro* averaged about 16 % lower than the corresponding *in vivo* values, although the distributions of individual values overlap to a considerable extent. The lower power output in some *in vitro* preparations probably resulted from a deficit in force production. The adductor muscle is easily fatigued (Marsh *et al.* 1992). Only seven adductions during swimming

leads to a 20 % decline in peak power and a 10 % drop in average power (Marsh *et al.* 1992), a decrement in performance that matches that occurring in our *in vitro* measurements. Although we allowed a recovery period following dissection and corrected for decreases in force during the experiments (Materials and methods), the initial force obtained *in vitro* may have been low because of fatigue occurring during the dissection. The *in vitro* preparations performed better at warmer temperatures, and at 20 ˚C the *in vitro* data were indistinguishable from the *in vivo* data collected at the same temperature (R. L. Marsh and J. M. Olson, unpublished results). This improved performance at warmer temperatures *in vitro* may indicate better recovery following the dissection. Despite the small quantitative deficit in performance of some *in vitro* preparations at 10 ˚C, the agreement between the two methods is quite impressive.

The force–velocity trajectory

We also measured the isotonic force–velocity curve for each muscle preparation used in these experiments (Olson and Marsh, 1993). Having the isotonic data makes it possible to examine to what extent these muscles operate on their force–velocity curves under *in vivo* conditions. Many authors have followed the lead of A. V. Hill (1938) and related mechanical power output *in vivo* to the isotonic force–velocity curve (e.g. Goldspink, 1977; Edgerton *et al.* 1986; Rome, 1990). This curve predicts that mechanical power will be optimized at an intermediate range of velocities and forces, and Hill (1950) and others (Wilkie, 1959; Goldspink, 1977; McMahon, 1984; Edgerton *et al.* 1986; Rome, 1990) have predicted that locomotor muscles will usually be designed by evolution to operate near this optimum in power production. However, muscles operating during locomotion probably rarely experience conditions that simulate those occurring during isotonic measurements *in vitro*. Loading conditions *in vivo* are complex and result from interactive effects of mechanical constraints and multiple intrinsic properties of the muscles (Josephson, 1981, 1985; Marsh, 1990). Because of these complexities, recent attempts to predict *in vivo* mechanical performance based on *in vitro* properties have incorporated additional kinetic parameters based on *in vitro* isometric properties, including length–tension effects and the kinetics of force development and relaxation (Caldwell and Chapman, 1989; Kaufman *et al.* 1991; van Leeuwen, 1992). Often not included, however, are known phenomena that are harder to model, such as shortening-induced deactivation and the effects of stretch (Edman *et al.* 1978; Edman, 1980; Housmans *et al.* 1983; Josephson and Stokes, 1988). Although various authors have suggested that there might be differences between the steady-state behavior of skeletal muscle and its behavior during natural movements (Josephson, 1985; Iwamoto *et al.* 1990), the present study provides the first accurate quantification of the force–velocity trajectory under natural conditions.

Because the scallop adductor required time at the beginning of shortening for activation events and the transition of cross-bridge states to occur, force and velocity initially increased simultaneously during simulated swimming (Fig. 9A). The force–velocity trace intersected the isotonic curve 38 ms after the stimulus. Of this 38 ms, approximately 20 ms was occupied by the latent period, during which no force was produced (Olson and Marsh, 1993). As velocity continued to increase, force remained

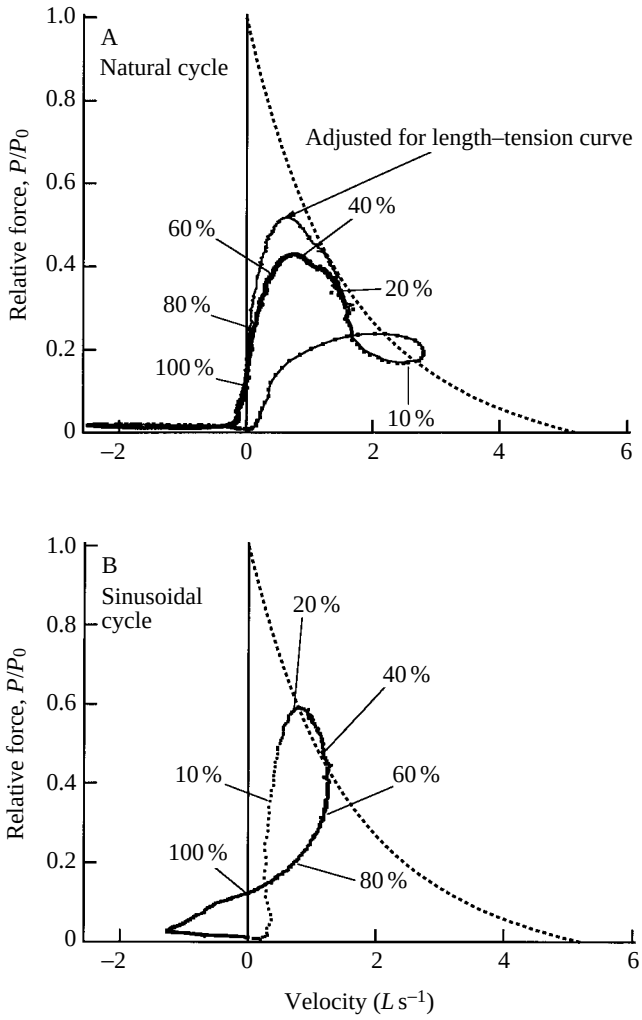

Fig. 9. Force–velocity trajectories of an adductor muscle from *Argopecten irradians* during the second cycle of repetitive contractions. Also plotted on the same axes is the force–velocity curve recorded in afterloaded isotonic tetanic contractions for the same muscle preparation (for methods, see Olson and Marsh, 1993). The points marked indicate time as a percentage of the total time required for shortening. (A) A cycle replicating the *in vivo* cycle. Two force–velocity trajectories are shown, one of which has been corrected for the decline in maximum isometric stress (P_0) predicted by the isometric length–tension curve (Olson and Marsh, 1993). This correction was applied by calculating P/P_0 using a P_0 appropriate for the length at each point in the cycle. (B) A sinusoidal cycle.

briefly higher than would be expected from the isotonic measurements. This excess force may result from a larger number of cross-bridges attached than occurs during steady shortening and/or elastic recoil of the muscle fibers (Iwamoto *et al.* 1990). The adductor muscle is attached directly to the two valves and thus has no series elastic elements

external to the fibers. Any elasticity is restricted to that present in the fibers themselves. Subsequently, force fell below the isotonic level as velocity decreased. After peak force had been reached, both force and velocity declined as the muscle was progressively deactivated. Force continued to fall and remained low during lengthening, as noted above. The differences between the isotonic force–velocity curve and that found under simulated *in vivo* conditions were probable largely due the transient nature of activation (Malamud and Josephson, 1991) during the cyclic contractions that characterize swimming. Additionally, because substantial shortening occurs, some of the deficit in force may have been caused by length–tension effects. If one assumes that the force–velocity curve shifted in concert with the decline in maximum isometric stress (P_0) during shortening, then the forces were somewhat closer to those predicted by the isotonic curve (Fig. 9A).

The isotonic force–velocity curve plots the peak velocity obtained during tetanic contractions, whereas the force–velocity trajectory follows these values continuously during shortening following a single stimulus. That the muscle operates on or above the isotonic curve for a portion of the force–velocity trajectory would appear to indicate that the muscle is fully activated by a single stimulus. In this context, the high ratio of twitch force to tetanic force found in the adductor muscle is noteworthy. The adductor muscle functioned near the isotonic curve for only approximately 30–40 % of the time required for shortening (Fig. 9A). (About 60 % of the total shortening occurred during this time.) Because the actual force was less than the force predicted from the isotonic curve for much of the shortening phase, the muscle produces approximately 25 % less power during shortening than would be predicted by assuming that it operates on the isotonic curve. The excellent agreement between *in vivo* and *in vitro* measurements of power output give us confidence that they reflect the behavior during normal locomotion. Clearly, the isotonic force–velocity curve should be interpreted as providing the approximate boundary conditions for the force–velocity trajectory during shortening and not as determining performance in a straightforward manner.

Comparison of the natural cycle with sinusoidal movements

We did not examine as many variations of sinusoidal cycles as in some previous studies because our main purpose was to examine power output using a length trajectory that matched the *in vivo* conditions. Nevertheless, some characteristics of ‘optimal’ sinusoidal cycles apparently corresponded approximately to those found in natural movements, including the frequency, strain and stimulus phase. The relatively large strain (22.5 %) found in this muscle both *in vivo* and in optimized sinusoidal contractions is noteworthy, as is the observation that the muscle length *in vivo* rarely exceeds L_0. The largest ‘optimal’ strain found *in vitro* with sinusoidal length changes in other skeletal muscles is 13 % (Altringham and Young, 1991). An optimal strain similar to that of scallop adductor has been reported for isolated ventricular trabeculae from frog heart, but at a considerably lower frequency (Syme, 1993). In all but one (Josephson and Stokes, 1988) of the previous investigations of cyclic work in skeletal muscle, the strain imposed has been symmetrical around L_0 and, thus, as strain is increased so is the degree of stretch above L_0. The available data leave open the question of whether the larger optimal strain found

in the scallop adductor is a peculiar characteristic of this muscle or whether larger optimal strains may be found in other muscles if they are allowed to begin shortening closer to L_0.

The distribution of power during sinusoidal length changes was unlike that found during swimming (Fig. 7). This results from a force–velocity trajectory during sinusoidal cycles that was distinctly different from that found in natural cycles (Fig. 9). Low velocity limited power output early in sinusoidal cycles even though force rose quickly. Peak power occurred as force was declining and was higher than that predicted by the force–velocity curve. Force was higher at the end of shortening than during the 'natural' cycle, resulting in negative work early in lengthening. Despite these differences, the overall performance was similar during the two types of cycles (Table 1). Nevertheless, the distribution of power during shortening undoubtedly influences animal performance. For example, in the escape movement of scallops, the high power output very early in adduction will aid rapid acceleration of the animal away from a predator.

In conclusion, power output during movement depends on the length trajectory as well as on the factors previously quantified during sinusoidal cycles, e.g. contractile frequency, strain and the phase and duration of stimulation. Defining the optimal length trajectory for average power during cyclic contractions must await further investigation, but quite different trajectories may result in similar average power. During movement, such as valve adduction in scallops, the biomechanics of the animal interact with the properties of the muscles to determine the shortening velocity, and optimizing average power output may not always be relevant to *in vivo* function. The complex nature of the force–velocity trajectory and its dependence on the shape of the length cycle suggest that interpreting kinematic data recorded *in vivo* in terms of the force–velocity curve should be approached cautiously. We have shown that, with sufficiently precise knowledge regarding the *in vivo* kinematics of a muscle and its stimulation regime, power output can be measured accurately *in vitro*. This technique will be particularly useful in examining the performance of muscles in which force and shortening cannot be measured simultaneously *in vivo*, and has recently been used in this context (Rome *et al.* 1993).

We thank S. K. Guzik for help with an initial set of measurements on scallop muscle. S. E. Marsh, G. S. Olson and A. J. Olson provided assistance with recording electromyograms. Supported by a grant from the National Institute of Arthritis and Musculoskeletal Diseases (AR-39318) to R.L.M. and a Biomedical Research Support Grant from the NIH to Northeastern University.

References

ALTRINGHAM, J. D. AND JOHNSTON, I. A. (1990). Modelling muscle power output in a swimming fish. *J. exp. Biol.* **148**, 395–402.

ALTRINGHAM, J. D. AND YOUNG, I. S. (1991). Power output and the frequency of oscillatory work in mammalian diaphragm muscle: the effects of animal size. *J. exp. Biol.* **157**, 381–389.

CALDWELL, G. E. AND CHAPMAN, A. E. (1989). Applied muscle modelling: implementation of muscle-specific models. *Comput. Biol. Med.* **19**, 417–434.

DAKIN, W. J. (1909). *Liverpool Marine Biology Committee, Memoirs on Typical British Marine Plants and Animals*, vol. XVII, Pecten (ed. W. A. Herdman). London: Williams and Norgate.

EDGERTON, V. R., ROY, R. R., GREGOR, R. J. AND RUGG, S. (1986). Morphological basis of skeletal

muscle power output. In *Human Muscle Power* (ed. N. L. Jones, N. McCartney and A. L. McComas), pp. 43–64. Champaign, IL: Human Kinetics Publishers.

EDMAN, K. A. P. (1980). Depression of mechanical performance by active shortening during twitch and tetanus of vertebrate muscle fibres. *Acta physiol. scand.* **109**, 15–26.

EDMAN, K. A. P., ELZINGA, G. AND NOBLE, M. I. M. (1978). Enhancement of mechanical performance by stretch during tetanic contractions of vertebrate skeletal muscle fibres. *J. Physiol., Lond.* **281**, 139–155.

GOLDSPINK, G. (1977). Mechanics and energetics of muscle in animals of different sizes, with particular reference to the muscle fibre composition of vertebrate muscle. In *Scale Effects in Animal Locomotion* (ed. T. J. Pedley), pp. 37–55. New York: Academic Press.

HILL, A. V. (1938). The heat of shortening and the dynamic constants of muscle. *Proc. R. Soc., Lond. B* **126**, 136–195.

HILL, A. V. (1950). The dimensions of animals and their muscular dynamics. *Science Progress* **38**, 209–230.

HILL, A. V. (1970). *First and Last Experiments in Muscle Mechanics*. Cambridge: Cambridge University Press.

HOUSMANS, P. R., LEE, N. K. M. AND BLINK, J. R. (1983). Active shortening retards the decline of the intracellular calcium transient in mammalian heart muscle. *Science* **221**, 159–161.

IWAMOTO, H., SUGAYA, R. AND SUGI, H. (1990). Force velocity relation of frog skeletal muscle fibres shortening under continuously changing load. *J. Physiol., Lond.* **422**, 185–202.

JONES, N. L., MCCARTNEY, N. AND MCCOMAS, A. J. (1986). *Human Muscle Power*. Champaign, IL: Human Kinetics Publishers.

JOSEPHSON, R. K. (1981). Temperature and the mechanical performance of insect muscle. In *Insect Thermoregulation* (ed. B. Heinrich), pp. 20–44. New York: Wiley.

JOSEPHSON, R. K. (1985). Mechanical power output from striated muscle during cyclic contraction. *J. exp. Biol.* **114**, 493–512.

JOSEPHSON, R. K. AND STOKES, D. R. (1988). Strain, muscle length and work output in a crab muscle. *J. exp. Biol.* **145**, 45–61.

KAUFMAN, K. R., AN, K. N., LITCHY, W. J. AND CHAO, E. Y. S. (1991). Physiological prediction of muscle forces. I. Theoretical formulation. *Neurosci.* **40**, 781–792.

LEHMAN, W. AND SZENT-GYÖRGYI, A. G. (1975). Regulation of muscular contraction: distribution of actin control and myosin control in the animal kingdom. *J. gen. Physiol.* **66**, 1–30.

LOWY, J. (1954). Contraction and relaxation in the adductor muscles of *Pecten maximus*. *J. Physiol., Lond.* **124**, 100–105.

MACHIN, K. E. AND PRINGLE, J. W. S. (1960). The physiology of insect fibrillar muscle. III. The effects of sinusoidal changes in length on beetle flight muscle. *Proc. R. Soc., Lond. B* **152**, 311–330.

MALAMUD, J. G. AND JOSEPHSON, R. K. (1991). Force–velocity relationships of a locust flight muscle at different times during a twitch contraction. *J. exp. Biol.* **159**, 65–87.

MARSH, R. L. (1990). Deactivation rate and shortening velocity as determinants of contractile frequency. *Am. J. Physiol.* **259**, R223–R230.

MARSH, R. L., OLSON, J. M. AND GUZIK, S. K. (1992). Mechanical performance of scallop adductor muscle during swimming. *Nature* **357**, 411–413.

MCMAHON, T. A. (1984). *Muscles, Reflexes and Locomotion.* Princeton, NJ: Princeton University Press.

MELLON, D., JR (1968). Junctional physiology and the motor nerve distribution in the fast adductor muscle of the scallop. *Science* **160**, 1018–1020.

MELLON, D., JR (1969). The reflex control of rhythmic motor output during swimming in the scallop. *Z. vergl. Physiol.* **62**, 318–336.

OLSON, J. M. AND MARSH, R. L. (1993). Contractile properties of the striated adductor muscle in the bay scallop *Argopecten irradians* at several temperatures. *J. exp. Biol.* **176**, 175–193.

ROME, L. C. (1990). The influence of temperature on muscle recruitment and function *in vivo*. *Am. J. Physiol.* **259**, R210–R222.

ROME, L. C., SWANK, D. AND CORDA, D. (1993). How fish power swimming. *Science* **261**, 340–343.

SIMMONS, R. M. AND SZENT-GYÖRGYI, A. G. (1985). A mechanical study of regulation in the striated adductor muscle of the scallop. *J. Physiol., Lond.* **358**, 47–64.

STEVENSON, R. D. AND JOSEPHSON, R. K. (1990). Effects of operating frequency and temperature on mechanical power output from moth flight muscle. *J. exp. Biol.* **149**, 61–78.

SYME, D. A. (1993). Influence of extent of muscle shortening and heart rate on work from frog heart trabeculae. *Am. J. Physiol.* **265**, R310–R319.

VAN LEEUWEN, J. L. (1992). Muscle function in locomotion. In *Advances in Comparative and Environmental Physiology*, vol. 11, *Mechanics of Animal Locomotion* (ed. R. McN. Alexander), pp. 191–250. Berlin: Springer-Verlag.

WEIS-FOGH, T. AND ALEXANDER, R. MCN. (1977). The sustained power output from striated muscle. In *Scale Effects in Animal Locomotion* (ed. T. J. Pedley), pp. 511–525. New York: Academic Press.

WILKENS, L. A. (1981). Neurobiology of the scallop. I. Starfish mediated escape behaviours. *Proc. R. Soc. Lond. B* **211**, 341–372.

WILKIE, D. R. (1959). Work output of animals: flight by birds and by man-power. *Nature* **183**, 1515–1516.

YONGE, C. M. (1936). The evolution of the swimming habit in the Lamellibranchia. *Mem. Musée R. Hist. Nat. Belg.* **3**, 77–100.